A genome-wide CRISPRi screen reveals a StkP-mediated connection between cell-wall integrity and competence in *Streptococcus salivarius*

Adrien Knoops[a], Alexandra Waegemans[a], Morgane Lamontagne[a], Baptiste Decat[a], Johann Mignolet[a,b], Jan-Willem Veening[b], Pascal Hols[a#]

[a] Louvain Institute of Biomolecular Science and Technology, Biochemistry and Genetics of Microorganisms, Université catholique de Louvain, Louvain-La-Neuve, Belgium

[b] Department of Fundamental Microbiology, Faculty of Biology and Medicine, University of Lausanne, Lausanne, Switzerland

[#] Address correspondence to Pascal Hols, Pascal.Hols@uclouvain.be

Running head

Competence-cell wall interplay in streptococci

Keywords

Cell-to-cell communication, genome-wide screen, quorum sensing, DNA transformation, ComRS, cell-wall, CRISPRi, serine-threonine kinase.

Word counts
Abstract: 180
Importance: 124
Main text: 5,600

This file contains
Main text
Table 1 to 3
Figure 1 to 6

ABSTRACT

Competence is one of the most efficient bacterial evolutionary and adaptative strategies by synchronizing production of antibacterial compounds and integration of DNA released by dead cells. In most streptococci, this tactic is orchestrated by the ComRS system, a pheromone communication device providing a sharp time window of activation in which only part of the population is responsive. Understanding how this developmental process integrates multiple inputs to fine-tune the adequate response is a long-standing question. However, essential genes involved in the regulation of ComRS have been challenging to study. In this work, we built a conditional mutant library using CRISPR-interference and performed three complementary screens to investigate competence genetic regulation in the human commensal *Streptococus salivarius*. We show that initiation of competence increases upon cell-wall impairment, suggesting a connection between cell envelope stress and competence activation. Notably, we report a key role for StkP, a serine-threonine kinase known to regulate cell-wall homeostasis. We show that StkP controls competence by a mechanism that reacts to peptidoglycan fragments. Together, our data suggest a key cell-wall sensing mechanism coupling competence to cell envelope integrity.

IMPORTANCE

Survival of human commensal streptococci in the digestive tract requires efficient strategies which must be tightly and collectively controlled for responding to competitive pressure and drastic environmental changes. In this context, the autocrine signaling system ComRS controlling competence for natural transformation and predation in salivarius streptococci could be seen as a multi-input device integrating a variety of environmental stimuli. In this work, we revealed novel positive and negative competence modulators by using a genome-wide CRISPR-interference strategy. Notably, we highlighted an unexpected connection between bacterial envelope integrity and competence activation that involves several cell-wall sensors. Together, these results showcase how commensal streptococci can fine-tune the pheromone-based competence system by responding to multiple inputs affecting their physiological status in order to calibrate an appropriate collective behavior.

INTRODUCTION

In the human digestive tract, bacteria face highly competitive pressure and physicochemical challenges. Surviving in this environment requires powerful and efficient strategies which must be tightly controlled and collectively coordinated (1-3). Quorum sensing (QS) devices are particularly suited to control concerted survival tactics since they perform bacterial density sensing. Initially thought to be restricted to this role, recent evidences suggest that QS systems can operate as autocrine modules and process multiple inputs (4). On the one hand, QS autocrine signaling allows heterogeneity amplification by positive feedback loops, a key feature for sub-populations activation (5-7). On the other hand, environmental stimuli can fine-tune the sensitivity of the pheromone-based apparatus (8, 9). This latter property is switching the QS property from a cell-density to a multi-input device, integrating diverse stimuli to calibrate population-wide strategies (4).

One of the best characterized QS-mediated process in Gram-positive bacteria is competence regulation (10). Orchestrating predation through bacteriocin production together with natural transformation, competence is regulated by two types of signaling systems in streptococci (11). The ComCDE system found in the mitis and anginosus groups relies on the sensing of the extracellular pheromone CSP (competence stimulating peptide) that induces a phosphorelay leading to transcriptional activation of competence genes comprising *comX*, which codes for the master competence-specific sigma factor (12). The alternative predominant system in streptococci is based on the production/maturation of the pheromone XIP (*comX*-inducer peptide), which is internalized by the Opp transporter and binds the intracellular receptor ComR (13, 14). Subsequently, the dimeric ComR·XIP complex activates several bacteriocin and competence genes including *comX* (15-17).

Uncovering the environmental triggers allowing permissive conditions for competence QS has remained challenging in streptococci (18). Since two-component systems (TCS) and serine-

86 threonine kinases (STK) are dedicated to sense the outside world, they constitute attractive
87 targets to couple environmental stimuli to QS reactivity. In *Streptococcus pneumoniae,* several
88 of those sensors (e.g. StkP, CiaRH, VicRK) have been highlighted to control the ComCDE
89 activity upon pH, O_2, cell density or antibiotic stresses (9, 19-23). In the cariogenic
90 *Streptococcus mutans* species, other distal regulators have been highlighted such as ScnRK,
91 HdrM, BrsRM, CiaRH or StkP that link competence activation to various growth conditions
92 (pH, carbohydrate source, oxygen, cell density) (24-31). In salivarius streptococci, we recently
93 uncovered a regulatory inhibition of the CovRS environmental sensor on the ComRS signaling
94 system (7). As exemplified by these three cases, despite the fact that environmental triggers can
95 be shared, environmental sensors bridging detection of stimuli to competence can be highly
96 divergent between species.

97 To investigate key sensors generating permissive conditions for competence activation,
98 genome-wide screens are the fastest and most-suited approaches. While Tn-seq strategies have
99 already revealed several regulators in *S. mutans* and *S. pneumoniae* (32, 33), classical knock-
100 out characterization of the identified genes is often impaired by their essentiality. Recently, a
101 genome-wide CRISPR-interference (CRISPRi) screening method was shown to overcome this
102 drawback for *Escherichia coli* and *S. pneumoniae* (34-36). This technique combines the use of
103 a guide RNA (gRNA) library targeting the whole genome together with a catalytically dead
104 mutant of Cas9 (dCas9), producing transcriptional interference upon DNA binding. Plugging
105 the dCas9 under the control of an inducible promoter allows the construction of a conditional
106 mutant library which can be used for genetic screens and further for characterization of essential
107 genes by knocking down their expression (34, 35).

108 In this work, we used this technique in combination with three distinct screens to unveil novel
109 competence regulators. Cross-validation of the hits obtained from the three screens converged
110 towards a connection between impairment of cell-wall biogenesis and competence activation.

111 Coherently, several sensors of the bacterial envelope integrity were identified among which
112 StkP, suggesting a putative signaling pathway bridging cell-wall stress to competence
113 activation.

114

RESULTS

Screening for spontaneous transformation by genome-wide CRISPRi inhibition

To identify unknown modulators of competence in *S. salivarius* HSISS4 (37), we set up a genome-wide CRISPRi strategy. To design gRNAs on the whole genome of HSISS4, we subset all the 20 nt sequences followed by a protospacer adjacent motif (PAM, NGG sequence) and retained only gRNAs binding the coding strand (non-template strand) of coding sequences (CDSs) and both strands in intergenic regions (34). We ended up with a total of 83,103 gRNAs (Table S1A) that were introduced under the control of a constitutive promoter (P_3, (38)) at a neutral chromosomal locus. The random chromosomal distribution of gRNAs in the library was preliminary evaluated by the direct sequencing of 40 individual clones (Fig. S1A).

The transfer of the library was initially performed in a strain carrying an IPTG-inducible dCas9 (P_{F6}-*lacI;* P_{lac}-*dcas9*, (35)), which was previously validated for generating CRISPRi conditional mutants (7) (Fig. 1). To evaluate the functionality of the library, this first strain was screened for the activation of spontaneous natural transformation. We hypothesized that dCas9-mediated repression of genes involved in competence inhibition (i.e. antagonist genes) will result in spontaneous natural transformation and donor DNA integration. We activated the interference library by adding IPTG (dCas9 activation) to a liquid culture supplemented with donor DNA containing a chloramphenicol resistance cassette (Fig. 1A). We were able to isolate 16 candidates after 3 independent rounds of selection, all harboring a different gRNA (Table 1). In order to confirm the phenotype generated by these gRNAs, we back-transformed them individually into the original strain and assessed their transformability. Spontaneous transformation was confirmed for 10 candidates (Table 1). Importantly, this functional screen succeeded to identify two previously described negative effectors of competence acting on ComX or XIP stability (*clpC* and *pepF*, respectively) (39, 40).

Screening based on gRNA depletion

This strategy was based on the toxicity of competence overactivation in the strain HSISS4 (16). We assumed that repression of competence-antagonist genes would produce a fitness cost, resulting in pool depletion of gRNAs targeting the corresponding genes. To set up this strategy, a second screening strain was generated by introducing a supplemental construct consisting of a xylose-inducible *comR* gene (P_{xyl2}-*comR*), allowing a mild competence activation upon addition of xylose, a non-metabolizable sugar in *S. salivarius* (7) (Fig. 1B). After introducing the gRNA library into this strain, we spread it on three different solid culture conditions. The first condition without any inducer was used as control (mock). The second condition was induced with IPTG alone to activate the CRISPRi library (Ci) and the third condition was supplemented with IPTG and xylose to concomitantly activate the CRISPRi library and competence (Ci+C). We hypothesized that we could identify modulator genes of competence by comparing the depletion of gRNAs between conditions Ci and Ci+C. To this aim, we performed high-throughput next-generation sequencing (NGS) to quantify each gRNA abundance per condition (Table S1). We first evaluated the randomness and homogeneity of gRNA distribution without any selection pressure (mock) by visualizing the mapping of the gRNAs on the genome of HSISS4 (Fig. S1B). Validating our previous Sanger-sequencing data (Fig. S1A), we showed that 99.7% (82,864 out of 83,104) of gRNAs were cloned in the non-induced library with an unbiased distribution (Table S1B and Fig. S1C). We next used the MAGeCK algorithm (41) to compare depletion of gRNAs between two conditions. As expected, the analysis of gRNA depletion between Ci and mock conditions uncovered well-known essential genes in streptococci (Table S2, Fig. S2A), as well as competence-related genes (e.g. *covR*, *pepF*) whose inactivation was recently shown to be lethal in strain HSISS4 (7, 40). We next performed the same analysis for the comparison of condition Ci+C with the mock (Table S3, Fig. S2B) and plotted against each other the two scores obtained from the two

comparisons (i.e. Ci vs mock and Ci+C vs mock) (Fig. S3). As expected, depletion scores in the two comparisons displayed a high correlation showing that gene fitness (i.e. positive, neutral or negative) was conserved with or without competence activation (linear regression of R^2=0.97). However, several outliers were present. Because they represent genes differentially affected in-between two conditions, we analyzed the standardized residuals of the linear regression (Fig. 2A, Table S4). We set up an arbitrary cut-off at +2.5 and -2.5 to identify the most representative outliers. Several depleted gRNAs were found as targeting genes known as competence antagonists such as the *mecA* gene encoding the ComX adaptor of the Clp degradation machinery (standardized residuals < -2.5, Table 2) (42). Unexpectedly, many crucial genes for competence activation (*comR*, *amiACDEF*) or competence-based bacteriocin production/immunity (e.g. *slvX-HSISS4_01664* operon) also showed gRNA depletion (Table 2) (16). In the strain HSISS4, competence, bacteriocins, and bacteriocin-immunity genes are concomitantly activated through ComR (16). Therefore, those genes might have been selected because a reduced competence activation goes along with a lower immunity rate toward bacteriocins, ultimately leading to a high fitness cost. Indeed, since bacteriocin producers are present at high cell density on plates due to xylose-mediated competence activation, non-competent and immunity-deficient cells will be killed through the well-established fratricide process (43).

Screening based on β-galactosidase activity

The last screening strategy was based on β-galactosidase (β-Gal) activity that allows the colorimetric evaluation of competence activation level in individual clones on plates with low selective pressure. For this purpose, a strain was generated by plugging the promoter of *comX* in front of the native *lacZ* gene (P_{comX}-*lacZ*) together with a P_{comX} luciferase reporter system (P_{comX}-*luxAB*) into the dCas9 and xylose-inducible competence strain (Fig. 1C). We transformed the gRNA library into this genetic background and spread it onto M17GL plates

189 supplemented with IPTG, xylose, and X-gal for detection of β- Gal activity. We examined
190 ~94,000 isolated colonies, searching for white and dark blue phenotypes. While white
191 phenotype is associated to targeted genes required for competence activation, dark blue
192 phenotype is related to targeted genes repressing competence development. We next re-isolated
193 the selected colonies to confirm their phenotypes and ended up with 141 dark blue and 68 white
194 clones. We sequenced their gRNAs to identify the interference target and quantified their
195 inhibition effects on P_{comX} activation thanks to the P_{comX}-*luxAB* module present in the strain. To
196 this aim, we slightly overexpressed *comR* with xylose thanks to the P_{xyl2}-*comR* module and
197 induced the gRNA-based inhibition system by adding IPTG. We compared the specific
198 luciferase activity of all the selected clones to the initial strain harboring no gRNA. The
199 sequence of the gRNAs, their identified targets, and their fold-changes in P_{comX} activation are
200 displayed in Table S5.

201 Since both frequency of selected gRNAs targeting the same gene and fold-change in P_{comX}
202 activation were relevant features to identify new competence regulators, we combined those
203 two parameters in the same analysis. On one hand, we calculated the mean fold-change in P_{comX}
204 activation for all gRNAs targeting the same gene. On the other hand, we counted the number
205 of selected gRNAs targeting the same gene. In addition, we normalized the count by the total
206 expected number of gRNAs of the library targeting each defined gene to avoid any gene-size
207 bias (higher probability to encounter a gRNA targeting a high-size gene) (Table S6). We plotted
208 those two variables (activation fold-change vs normalized gRNA frequency) and validated the
209 screen by finding most of the proximal effectors of the ComRS system, i.e. *comR*, *amiACDEF*,
210 *clpC* and P_{comX} (Fig. 2B and Table S6) (7, 16, 42). We next applied an arbitrary cut-off
211 (normalized count > 0.02 and $\log_2$(FC) > 0.5) to find the most significant genes with an
212 antagonist function towards competence (Table 3). We thereby selected several players whose
213 role in competence inhibition was also suggested with the gRNA depletion screen, such as the

phosphate transporter system (*pstC1*) and the serine-threonine kinase (*stkP*) genes. Strikingly, the mannose/glucosamine PTS transporter operon (*manLMN*) was particularly overrepresented, even though absent from the two previous screens. This result might be an artefactual consequence of a carbon metabolism shift enhancing xylose uptake ultimately resulting in higher *comR* induction, but could also be due to a link between mannose catabolism and competence as reported in *S. mutans* (30).

Cell-wall integrity is a signal for competence

Since many genes were identified to affect competence by the three screening approaches, we used the Clusters of Orthologous Genes (COG) database (44) to classify them by general function. For this analysis, we selected only the genes whose inhibition is expected to induce competence (i.e. all the genes from the transformation screen, genes with standardized residuals < -2.5 from the growth screen, and genes with $\log_2(FC) > 0.5$ and normalized count > 0.02 from the colorimetric screen). We next assessed the importance of the different pathways for competence activation. For this purpose, we counted the number of genes per screen involved in one COG function and normalized it by the total number of genes within this COG function in the HSISS4 genome (Fig. 3A). This analysis indicated that the most represented function was cell wall/membrane/envelope biogenesis (23% of all the genes highlighted vs ~5% at the whole genome level). Furthermore, we observed that overlapping genes between gRNA depletion and β-Gal screens were all directly or indirectly involved in cell-envelope assembly. Indeed, we identified in both screens the *dltA* and *dltB* genes involved in teichoic acid D-alanylation (45), the phosphoglucomutase *pgmA* gene involved in the biosynthesis of extracellular polysaccharides (46), the cell wall-related serine-threonine kinase *stkP* gene (47, 48), and the phosphate transporter *pstC1* gene with an important role for poly(glycerophosphate) teichoic acid synthesis (49) (Fig. 3B).

We next drew a more precise view of the different cell wall pathways targeted by gRNA that presumably lead to competence activation. We found that genes involved in the synthesis of peptidoglycan, teichoic acids, and extracellular polysaccharides were all affected (Fig. 4). In parallel, key sensors (StkP, LiaFSR) or mediators (SpxA1) known to be triggered by cell wall alterations were also identified in the screens (24, 50-54), suggesting a possible link between cell wall integrity and ComRS activation.

StkP controls *comX* expression through muropeptide binding

Since StkP was highlighted in two screens with multiple different gRNAs and is cell wall-associated, we decided to further investigate its link with competence activation. Serine-threonine kinases are pleiotropic regulators that control key cellular processes such as dormancy, virulence, cell division, and cell wall synthesis through protein phosphorylation (47, 48). In *S. salivarius*, only one serine-threonine kinase homolog is present and displays PASTA motifs shown to bind muropeptides in *Bacillus subtilis* (55). Besides, StkP of *S. pneumoniae* has been shown to coordinate cell wall synthesis and septation (24, 56-58) while an unclear link with competence has been suggested in *S. mutans* and *S. pneumoniae* (19, 23, 24).

In a first set of experiments, we transferred a gRNA targeting *stkP* in a strain harboring the dCas9 module (P_{F6}-*lacI* P_{lac}-*dcas9*) together with a luciferase reporter of the transcriptional activity of *comR* (P_{comR}-*luxAB*) or *comX* (P_{comX}-*luxAB*) and the xylose-inducible module allowing competence activation (P_{xyl2}-*comR*). Monitoring activation of those two promoters with or without *stkP* inhibition suggested that StkP level influences *comX* expression but has no impact on *comR* transcription (Fig. 5A). We next used the same *comX* reporter strain with increasing xylose concentrations for *comR* induction and measured P_{comX} activation with or without *stkP* inhibition (Fig. 5B). Stronger inhibitions of *stkP* were recorded for lower ComR levels, suggesting that ComR overproduction interferes with the StkP-mediated regulation of *comX*.

Since StkP was shown to bind specific muropeptides via its PASTA domains (55), we investigated if the addition of peptidoglycan extracts was able to modulate competence. To this aim, we purified peptidoglycan from *S. salivarius* (L-Lys pentapeptide) or *B. subtilis* (Meso-DAP pentapeptide) and measured the activation of the P_{comX}-*luxAB* reporter strain with (-| *stkP*) or without (mock) dCas9 interference on *stkP* expression (Fig. 5C). While *S. salivarius* peptidoglycan could decrease P_{comX} activation, *B. subtilis* extracts (negative control) did not result in a significative reduction. Moreover, adding peptidoglycan from *S. salivarius* prevented P_{comX} repression when *stkP* was inhibited, suggesting that StkP mediates the signalization (Fig. 5D).

Altogether, these results suggest that StkP interferes with the transcriptional activity of the ComR·XIP complex by an unknown mechanism, which is modulated by the binding of specific muropeptides.

DISCUSSION

How QS modules integrate multiple inputs to fine-tune their sensitivity and optimize collective behavior is a challenging topic. In this work, we performed a genome-wide screen coupled to three different readouts to uncover key triggers of ComRS-mediated competence activation. Using a conditional mutant library, we highlighted a connection between cell wall biogenesis and competence activation. Moreover, we uncovered a link between muropeptide sensing via the serine threonine StkP and competence development. Those pieces of evidence suggest a key role of cell wall stress on the competence response (Fig. 6).

To discover novel players involved in competence regulation, we built a CRISPRi-based library and performed three types of screen in parallel. The interference technology offers several advantages over the classical random transposon mutagenesis (59) but the primary one is the production of conditional mutants allowing the study of essential/deleterious genes. Considering the transformation screen, the library was transiently induced, dampening the toxic-acquired phenotype due to constitutive activation of natural transformation. This strategy provided a direct screening method for DNA integration and allowed us to select gRNAs targeting essential genes among which *pepF*, a gene essential for competence shut-off recently discovered in *S. salivarius* (40). In addition, we also selected two different gRNAs targeting *clpC*, a gene encoding a component of the MecA-ClpCP machinery responsible for ComX degradation (39, 60). Those results confirm the roles of PepF and ClpC to prevent spontaneous competence activation at the early and late stage of competence, respectively (40, 42, 60). Moreover, novel competence modulators were identified such as a putative bactoprenol glucosyltransferase and 3 hypothetical proteins. Specifically, interference on the putative bactoprenol glucosyltransferase resulted in a high transformation rate (~10^{-2}, Table 1), suggesting an important role of this player for competence control. Although the transformation screen displays interesting features to select essential genes connected to competence

development, it would require a massive number of cells to ensure a complete coverage of the high-density gRNA library. This issue is not present in the gRNA depletion screen, where high-throughput NGS is exploited to map and quantify all the gRNAs, generating a complete picture at the genome scale. Nevertheless, the identification of the genes is based on the competence-related toxic phenotype. This feature could limit the detection of essential genes whose inhibition has a high fitness cost. Of note, the competence-associated toxicity used in the gRNA depletion screen could explain some intriguing results. While NGS data showed a depletion of gRNAs targeting genes involved in the downregulation of competence such as *mecA*, the depletion of gRNAs targeting crucial genes for competence activation (e.g. *comR* or the *ami/opp* operon) was counterintuitive. To reconcile these findings, we reasoned that a lack of functional competence goes along with an impairment in bacteriocin immunity. Consequently, the gRNA depletion will also include bacteriocin/immunity loci and key players required for competence activation (Table 2 and Table S3). Finally, as the colorimetric β-gal test is based on P_{comX} activity and visual selection, this screen drastically reduces any fitness bias. To sum up, this work highlights the added value of combining different screening approaches to unveil the largest set of candidate genes connected to competence control.

The three screens converge to select gRNAs involved in key envelope biogenesis processes and its control by cell wall sensors (Fig. 4). The connection between cell wall and competence has only been reported in a similar experiment with Tn-seq in *S. mutans* (61). However, the authors report that inactivation by transposon insertion of the cell wall related genes *pknB* (homolog of *stkP*), *rgpL*, *dltA* and *liaS* results in a lower activation of competence, contrasting with the results obtained in this study. Opposite effects of competence regulators in *S. salivarius* and *S. mutans* have already been reported for the CovRS system (7, 62) and showcase that species have evolved control mechanisms in line with their own lifestyles. Aside from the cell wall synthesis, several other pathways were highlighted (Fig. 6). One of them is translation, with

several important players targeted (rRNAs, tRNAs, peptide chain release factor, ribosomal proteins, and tRNA synthetases). This correlation is interesting in the light of the work of Stevens and coworkers, who showed that translation fidelity impairment promotes competence activation in *S. pneumoniae* (63). In addition, important genes involved in chromosome replication/segregation (*priA*, *cshA/rarA*, *scpB*) and DNA repair (*mutL*, *mutT*, *dinP*) were also underlined by the screens (Table 3, Tables S4 and S6). Replication stress was previously shown to induce pneumococcal competence, but the exact mechanism remains unclear and involves *comCDE* gene dosage control and/or a role for arrested and unrepaired replication forks (64, 65). The screens did highlight a role for enzymes or transporters involved in amino acid biosynthesis or uptake for arginine (CarB and ArgJ), glutamine (GlnP), glutamate (HSISS4_00833 and 00832) and leucine (LivJ). Amino acid starvation is known to trigger the stringent response via RelA and the production of (p)ppGpp alarmones (66), which was shown to influence competence regulation in *S. mutans* (67). Altogether, the screens performed here suggest that *S. salivarius* competence control relies on the sensing of various alterations of key metabolic/physiological functions, reinforcing the view that competence activation could be seen as a general stress response in streptococci.

In this work, we specifically investigate StkP, a key sensor of cell wall integrity in *S. pneumoniae* (54). In streptococci, StkP was also shown to phosphorylate classical response regulators of two-component systems such as the virulence regulator CovR in *Streptococcus agalactiae* and *Streptococcus pyogenes* (68, 69), the cell wall regulator VicR in *S. mutans* and *S. pneumoniae* (24, 54), and the competence regulator ComE in *S. pneumoniae* for which StkP phosphorylation triggers a distinct regulon from the aspartate phospho-transfer mediated by ComD (22). The pleiotropic effects of StkP and its involvement in major cellular processes is probably the reason why its impact on competence has been reported but remains controversial in *S. pneumoniae* (19, 22, 23). In *S. salivarius*, we showed that *stkP* depletion promotes a higher

351 *comX* activation without major effect on *comR* expression. This suggests a mechanism acting
352 directly on the ComR sensor by increasing its trans-activator properties. This hypothesis is
353 strengthened by the fact that ComR overexpression curtails the effect of StkP on *comX*
354 activation (Fig. 5B). The exact process remains to be discovered, even if it suggests a direct
355 effect of StkP on ComR. Two non-exclusive mechanisms could explain the control of
356 competence by StkP in *S. salivarius*. On one hand, the kinase could sense directly or indirectly
357 a disfunction in the cell wall synthesis. Beside a direct effect on ComR, this impairment could
358 also be transmitted to other cell wall sensors. Interestingly, two of these sensor systems (i.e.
359 VicRK and LiaSRF) were highlighted in the β-gal screen (Tables 3 and S5) and were previously
360 shown to affect competence activation in *S. salivarius* (Fig. 6) (7). On the other hand, the kinase
361 could also control competence as a muropeptide signaling system. Our experiments with
362 peptidoglycan extracts (Fig. 5C and D) advocate for this possibility as a high concentration of
363 self-muropeptides inhibits competence in a StkP-dependent manner. In line with this,
364 competence in streptococci is transiently activated during the early exponential growth but
365 could not be triggered in stationary phase when the extracellular muropeptide concentration is
366 expected to be high (14, 16, 70). This may suggest that StkP acts as a growth phase sensor to
367 extinct competence at high cell density (Fig. 6).

368 To conclude, we showed the large potential of combining a genome-wide CRISPRi strategy
369 with multiple screening approaches to connect essential genes involved in physiological
370 pathways to competence development. Besides the well-established ComRS-ComX regulatory
371 pathway, we revealed that disturbance of general functions such as cell envelope assembly,
372 amino-acid metabolism, translation, and replication modulates competence activation in *S.*
373 *salivarius*. This work strengthens our view that competence is a general adaptative response
374 that ensures survival in a broad range of stress conditions. Moreover, the identification of a
375 large set of “competence-associated” genes paves the way to understand novel regulatory

376 cascades interconnecting cell-proliferation impairment and competence activation such as
377 illustrated here for the role of the serine/threonine kinase StkP in cell wall-mediated competence
378 modulation.

MATERIALS AND METHODS

Bacterial strains, plasmids, sgRNA and oligonucleotides

Bacterial strains, plasmids, sgRNA and oligonucleotides used in this study are listed and described in supplemental material (Tables S7A-D).

Growth conditions and competence induction

S. salivarius HSISS4 (71) and derivatives were grown at 37°C without shaking in M17 (Difco Laboratories, Detroit, MI) or in chemically-defined medium (CDM) (72) supplemented with 1% (w/v) glucose (M17G, CDMG, respectively). Chromosomal genetic constructions were introduced in *S. salivarius* via natural transformation (73). We added D-xylose (0.1 to 1%; w/v), IPTG (1 mM), spectinomycin (200 µg/ml), chloramphenicol (5 µg/ml) or erythromycin (10 µg/ml), as required. The synthetic peptides (purity of 95%), were supplied by Peptide 2.0 Inc. (Chantilly, VA) and resuspended first in dimethyl-formamide (DMF) and diluted in water to reach low DMF concentration (final of 0.02%). Solid plates inoculated with streptococci cells were incubated anaerobically (BBL GasPak systems, Becton Dickinson, Franklin lakes, NJ) at 37°C.

To induce competence, overnight CDMG precultures were diluted at a final OD_{600} of 0.05 in 500 µl of fresh CDMG and incubated 100 min at 37°C. Then, the pheromone sXIP (LPYFAGCL) and DNA (Gibson assembled PCR products or plasmids) were added and cells were incubated for 3 h at 37°C before plating on M17G agar supplemented with antibiotics when required.

Library design and construction

The gRNA library was designed by selecting all the 20 nt followed by a PAM sequence within the genome of HSISS4. Since it was shown that efficient interference in CDSs occurs only with gRNAs targeting the coding strand (34), we filtered the library to keep only gRNAs targeting the coding strand in CDSs and targeting both strands in intergenic regions. We ended up with

a high-density library of 83,104 gRNAs resulting in a theoretical base pairing every 25 pb on the HSISS4 genome. Of note, we chose to use a high-density library to target unknown small genetic elements such as siRNA or small peptides. We ordered the gRNAs as single strand DNA (Twist BioSciences) and amplified the oligo-pool thanks to common upstream and downstream region using primers AK475 and AK476. To reduce any amplification sequence-bias, we used 10 cycles of amplification.

The PCR products were then purified (Monarch kit, NEB) and Gibson-joined to the pre-amplified upstream homologous region of the neutral locus *gor* (downstream of *HSISS4_00325*) containing an erythromycin resistance gene and to the downstream homologous region of the same locus fused to a P_3 constitutive promoter. We performed 20 independent Gibson assemblies, which were latter transformed by natural transformation into 20 independent cultures of HSISS4 strains containing at least a lactose-inducible dCas9 module (P_{F6}-*lacI*; P_{lac}-*dcas9*) (7). Supplemental genetic constructions (P_{xyl2}-*comR*, P_{comX}-*lacZ*, P_{comX}-*luxAB*) were present in those strains depending on the screening strategy. For every library produced, we calculated the number of transformants to obtain at least 15-fold transformants over the diversity rate, ensuring theoretically that 99,9% of the diversity would be present in the library (74). We finally pooled all the transformants in Phosphate Buffered Saline (PBS, 137 mM NaCl, 2.7 mM KCl, 10 mM Na_2HPO_4, 1.8 mM KH_2PO_4) and measured OD_{600} prior to storage at -80°C.

CRISPRi transformation screen

For the spontaneous transformation screen, we first introduced the gRNA library in the lactose-inducible strain harboring a P_{comX} luciferase reporter system (P_{F6}-*lacI*, P_{lac}-*dcas9*, P_{comX}-*luxAB*). We next diluted the cells in 15 ml of fresh CDMG supplemented with IPTG 1 mM at an OD_{600} of 0.01. We grew this culture at 37°C for 8 h and added every 30 min a PCR-amplified product consisting of a chloramphenicol cassette with 2000-pb up and down homologous recombination

arms at a final concentration of 0.25 nM. We centrifugated this culture, plated it on chloramphenicol plates and grew it overnight. Colonies were picked and donor DNA integration was confirmed by PCR. We next amplified the locus containing the gRNAs before Sanger sequencing.

CRISPRi gRNA depletion screen

For the gRNA depletion analysis, we used the same strain as described in the previous section. After introducing the gRNAs in this background, we spread the resulting library onto three different solid media (M17G; M17G IPTG 100 µM; M17G IPTG 100 µM xylose 1%) resulting in an average of 9.6×10^6 CFU per large plate. Technical replicates (n = 4) were incubated 16 h at 37°C to yield an estimated mean of ~12 generations. Cells were then collected, pooled in PBS buffer and homogenized for each replicate. After genomic extraction (GenElute, Sigma Aldrich) from at least 1.5×10^9 CFU per replicate, we PCR-amplified the locus containing the gRNAs prior to their deep sequencing. We used an optimized PCR protocol with high primer concentration (5 µM), low template genomic DNA (2 ng/µl), and low number of cycles (15 cycles) to avoid any chimeric products due to the highly randomized gRNA sequences. The 219-pb amplicons were next gel-purified (Monarch DNA Gel Extraction kit, NEB) and sent with a minimum amount of 4 pmol for Illumina sequencing (GeneWiz). High-Seq Illumina sequencing was performed with 30% Phix and generated an average of 30 M reads per replicate. All gRNA sequencing data was deposited in the GEO database under accession number GSE204976.

CRISPRi β-galactosidase activity screen

We first produced a new genetic background by introducing into the strain described in the previous section an ectopic copy of *comR* under the control of a xylose-inducible promoter (P_{xyl2}-*comR*) together with a chloramphenicol resistance cassette at the neutral locus *suc* (upstream of *HSISS4_01641*). We next fused the promoter of *comX* to the native *lacZ* gene

(P_{comX}-*lacZ*) together with a spectinomycin resistance cassette and introduced the gRNA library into this strain. The resulting library was spread on M17 0.5% glucose, 0.5% lactose (M17GL), IPTG 100 µM, xylose 1%, and X-gal 100 mg/ml for screening dark-blue (highly competent) and white (competence loss) colonies. A total of 158 dark blue and 155 white clones from the screening of ~94,000 colonies were re-isolated for phenotype confirmation. Luciferase tests (P_{comX}-*luxAB*) were performed in comparison with the parental strain harboring no gRNA. Clones with the most dissimilar luciferase phenotypes (141 dark blue and 68 white clones) were selected and gRNAs were amplified by PCR for Sanger-sequencing.

NGS analysis

We used the MAGeCK algorithm to map the reads on the HSISS4 genome (41). Approximatively 30% of total reads were mapped, producing about 10 M reads per replicate. Following the MAGeCK guidelines, we next pooled the reads from the 4 replicates, ultimately generating a total of 40 M reads per condition. In a first analysis, we compared the gRNA depletion in the IPTG-induced condition with the mock to determine all the essential genes from strain HSISS4. For the sake of clarity, we only compared gRNAs targeting CDSs, since gRNAs targeting intergenic regions are much more complicated to determine. We next compared the depletion of gRNAs for each gene in the IPTG- and IPTG-xylose-induced conditions to the mock condition thanks to the MAGeCK algorithm. The depletion scores generated per gene for the two induced conditions were then plotted against each other and a linear regression was fitted to the plot (*lm* function, R package) and outliers were identified by standardizing the residuals.

COG analysis

The conserved domain database of NCBI was used to infer functions of the genes from the genome of HSISS4 (44, 75) and only the highest scored function for each gene were retained. The number of genes of the whole genome involved in each function prediction was then

calculated, generating a function prediction frequency matrix. This matrix was then used to weight the number of genes with a specific predicted function highlighted in the different screens.

Luciferase assay

Overnight precultures were diluted at a final OD_{600} of 0.05. A volume of 300 µl of culture was transferred in the wells of a sterile covered white microplate with a transparent bottom (Greiner, Alphen a/d Rijn, The Netherlands). These culture samples were supplemented with D-xylose, IPTG or peptidoglycan extracts if stated. Growth (OD_{600}) and luciferase (Lux) activity (expressed in relative light units, RLU) were monitored at 10 min intervals during 8 to 24 h in a Hidex Sense microplate reader (Hidex, Lemminkäisenkatu, Finland). Specific Lux activity were obtained by dividing Lux activity by the OD_{600} and summing all the data obtained over time. When stated, biological or technical triplicates were averaged. Statistical analyses of simple and multiple comparisons to the control mean were performed with *t*-test (unilateral distribution, heteroscedastic) and one-way ANOVA with Dunnett's test, respectively. For both, standard deviations and *P* values were calculated.

Transformation test

The CDMG preculture of HSISS4 and derivatives was diluted in 500 µl of CDMG supplemented with 1 mM IPTG at an OD_{600} of 0.005. The culture was grown at 37°C for 8 h and we added every 30 min a PCR-amplified product consisting of a chloramphenicol resistance cassette surrounded by up and down homologous recombination arms (2000 pb each) at a final concentration of 0.25 nM. We next performed serial dilution of the culture and spread the various dilutions on M17G plates supplemented with or without chloramphenicol 5 µg/ml. We next calculated the transformation rate based on the CFU numbers of the two plates.

Peptidoglycan extracts

503 Peptidoglycan extracts were prepared as previously reported (55). Cultures of 100 ml of *S.*
504 *salivarius* HSISS4 or *B. subtilis* 168 were grown to an OD_{600} of ~1.2 in M17 or LB media,
505 respectively. Cells were collected by centrifugation, washed with 0.8% NaCl, resuspended in
506 hot 4% SDS, boiled for 30 min, and incubated at room temperature overnight. The suspension
507 was then boiled for 10 min and the SDS-insoluble cell-wall material was collected by
508 centrifugation at 12,000 *g* for 15 min at room temperature. The pellet-containing cell wall
509 peptidoglycan was washed four times with water and finally resuspended in 1 ml sterile water.
510 The resuspended peptidoglycan was next digested with mutanolysin (10 µg/ml) overnight at
511 37°C prior to inactivation of mutanolysin at 80°C for 20 min.

512 **ACKNOWLEDGEMENTS**

513 The work of PH was supported by the Belgian National Fund for Scientific Research (FNRS,
514 grant PDR T.0110.18) and the Concerted Research Actions (ARC, grant 17/22-084) from
515 Federation Wallonia-Brussels. AK held a doctoral fellowship from FNRS (FRIA fellowship).
516 PH is Research Director at FNRS. The funders had no role in study design, data collection and
517 interpretation, or the decision to submit the work for publication.

518 We thank Marcello Mora for its advices on non-specific DNA amplification.

519 **AUTHOR CONTRIBUTIONS**

520 AK and PH conceived and designed the study. AK, AW, ML, BD, and JM carried the laboratory
521 work. AK, JWV, JM and PH analyzed and interpreted the data. AK, JWV, JM and PH wrote
522 and revised the manuscript. All authors read and approved the final manuscript.

523 **COMPETING INTERESTS**

524 The authors declare no conflict of interest.
525

SUPPLEMENTAL MATERIAL

Supplementary Figures:

Figure S1. Random chromosomal distribution of the gRNA library

Figure S2. Gene-associated gRNA depletion scores

Figure S3. Linear regression of gene-associated gRNA depletion scores

Supplementary Tables:

Table S1. List of oligonucleotides used for the genome-wide CRISPRi strategy
(separate .xls file)

Table S2. List of gene-associated gRNA depletion scores from library activation
(separate .xls file)

Table S3. List of gene-associated gRNA depletion scores from library and competence activation
(separate .xls file)

Table S4. List of competence-associated genes (standardized residuals) from the gRNA depletion screen
(separate .xls file)

Table S5. List of gRNA and their targeted genes from the β-Gal screen
(separate .xls file)

Table S6. List of normalized competence-associated genes from the β-Gal screen
(separate .xls file)

Table S7. List of bacterial strains (A), plasmids (B), oligonucleotides (C), and PCR fragments (D) used in this study

552 **REFERENCES**

553

554 1. Huang R, Li M, Gregory RL. 2011. Bacterial interactions in dental biofilm. *Virulence*
555 2:435-444.

556 2. Huttenhower C, Gevers D, Knight R, Abubucker S, Badger JH, Chinwalla AT, Creasy
557 HH, et al. 2012. Structure, function and diversity of the healthy human microbiome.
558 *Nature* 486:207-214.

559 3. Kommineni S, Bretl DJ, Lam V, Chakraborty R, Hayward M, Simpson P, Cao Y,
560 Bousounis P, Kristich CJ, Salzman NH. 2015. Bacteriocin production augments niche
561 competition by enterococci in the mammalian gastrointestinal tract. *Nature* 526:719-
562 722.

563 4. Bettenworth V, Steinfeld B, Duin H, Petersen K, Streit WR, Bischofs I, Becker A. 2019.
564 Phenotypic Heterogeneity in Bacterial Quorum Sensing Systems. *J Mol Biol* 431:4530-
565 4546.

566 5. Doganer BA, Yan LKQ, Youk H. 2016. Autocrine Signaling and Quorum Sensing:
567 Extreme Ends of a Common Spectrum. *Trends Cell Biol* 26:262-271.

568 6. Domenech A, Slager J, Veening JW. 2018. Antibiotic-Induced Cell Chaining Triggers
569 Pneumococcal Competence by Reshaping Quorum Sensing to Autocrine-Like
570 Signaling. *Cell Rep* 25:2390-2400.

571 7. Knoops A, Vande CF, Fontaine L, Verhaegen M, Mignolet J, Goffin P, Mahillon J, Sass
572 A, Coenye T, Ledesma-Garcia L, Hols P. 2022. The CovRS Environmental Sensor
573 Directly Controls the ComRS Signaling System To Orchestrate Competence Bimodality
574 in Salivarius Streptococci. *mBio* 13:e0312521.

575 8. Chang JC, Jimenez JC, Federle MJ. 2015. Induction of a quorum sensing pathway by
576 environmental signals enhances group A streptococcal resistance to lysozyme. *Mol*
577 *Microbiol* 97:1097-1113.

578 9. Moreno-Gamez S, Sorg RA, Domenech A, Kjos M, Weissing FJ, van Doorn GS,
579 Veening JW. 2017. Quorum sensing integrates environmental cues, cell density and cell
580 history to control bacterial competence. *Nat Commun* 8:854.

581 10. Neiditch MB, Capodagli GC, Prehna G, Federle MJ. 2017. Genetic and Structural
582 Analyses of RRNPP Intercellular Peptide Signaling of Gram-Positive Bacteria. *Annu*
583 *Rev Genet* 51:311-333.

584 11. Fontaine L, Wahl A, Flechard M, Mignolet J, Hols P. 2015. Regulation of competence
585 for natural transformation in streptococci. *Infect Genet Evol* 33:343-360.

586 12. Shanker E, Federle MJ. 2017. Quorum Sensing Regulation of Competence and
587 Bacteriocins in *Streptococcus pneumoniae* and *mutans*. *Genes (Basel)* 8:15.

588 13. Fontaine L, Boutry C, de Frahan MH, Delplace B, Fremaux C, Horvath P, Boyaval P,
589 Hols P. 2010. A novel pheromone quorum-sensing system controls the development of

590 natural competence in *Streptococcus thermophilus* and *Streptococcus salivarius*. *J*
591 *Bacteriol* 192:1444-1454.

592 14. Gardan R, Besset C, Gitton C, Guillot A, Fontaine L, Hols P, Monnet V. 2013.
593 Extracellular life cycle of ComS, the competence-stimulating peptide of *Streptococcus*
594 *thermophilus*. *J Bacteriol* 195:1845-1855.

595 15. Fontaine L, Goffin P, Dubout H, Delplace B, Baulard A, Lecat-Guillet N, Chambellon
596 E, Gardan R, Hols P. 2013. Mechanism of competence activation by the ComRS
597 signalling system in streptococci. *Mol Microbiol* 87:1113-1132.

598 16. Mignolet J, Fontaine L, Sass A, Nannan C, Mahillon J, Coenye T, Hols P. 2018.
599 Circuitry Rewiring Directly Couples Competence to Predation in the Gut Dweller
600 *Streptococcus salivarius*. *Cell Rep* 22:1627-1638.

601 17. Talagas A, Fontaine L, Ledesma-Garcia L, Mignolet J, Li de la Sierra-Gallay, Lazar N,
602 Aumont-Nicaise M, Federle MJ, Prehna G, Hols P, Nessler S. 2016. Structural Insights
603 into Streptococcal Competence Regulation by the Cell-to-Cell Communication System
604 ComRS. *PLoS Pathog* 12:e1005980.

605 18. Hagen SJ, Son M. 2017. Origins of heterogeneity in *Streptococcus mutans* competence:
606 interpreting an environment-sensitive signaling pathway. *Phys Biol* 14:015001.

607 19. Echenique J, Kadioglu A, Romao S, Andrew PW, Trombe MC. 2004. Protein
608 serine/threonine kinase StkP positively controls virulence and competence in
609 *Streptococcus pneumoniae*. *Infect Immun* 72:2434-2437.

610 20. Echenique JR, Chapuy-Regaud S, Trombe MC. 2000. Competence regulation by
611 oxygen in *Streptococcus pneumoniae*: involvement of ciaRH and comCDE. *Mol*
612 *Microbiol* 36:688-696.

613 21. Echenique JR, Trombe MC. 2001. Competence repression under oxygen limitation
614 through the two-component MicAB signal-transducing system in *Streptococcus*
615 *pneumoniae* and involvement of the PAS domain of MicB. *J Bacteriol* 183:4599-4608.

616 22. Pinas GE, Reinoso-Vizcaino NM, Yandar Barahona NY, Cortes PR, Duran R,
617 Badapanda C, Rathore A, Bichara DR, Cian MB, Olivero NB, Perez DR, Echenique J.
618 2018. Crosstalk between the serine/threonine kinase StkP and the response regulator
619 ComE controls the stress response and intracellular survival of *Streptococcus*
620 *pneumoniae*. *PLoS Pathog* 14:e1007118.

621 23. Saskova L, Novakova L, Basler M, Branny P. 2007. Eukaryotic-type serine/threonine
622 protein kinase StkP is a global regulator of gene expression in *Streptococcus*
623 *pneumoniae*. *J Bacteriol* 189:4168-4179.

624 24. Banu LD, Conrads G, Rehrauer H, Hussain H, Allan E, van der Ploeg JR. 2010. The
625 *Streptococcus mutans* serine/threonine kinase, PknB, regulates competence
626 development, bacteriocin production, and cell wall metabolism. *Infect Immun* 78:2209-
627 2220.

628 25. Dufour D, Cordova M, Cvitkovitch DG, Levesque CM. 2011. Regulation of the
629 competence pathway as a novel role associated with a streptococcal bacteriocin. *J*
630 *Bacteriol* 193:6552-6559.

631 26. Kim JN, Stanhope MJ, Burne RA. 2013. Core-gene-encoded peptide regulating
632 virulence-associated traits in *Streptococcus mutans*. *J Bacteriol* 195:2912-2920.

633 27. Levesque CM, Mair RW, Perry JA, Lau PC, Li YH, Cvitkovitch DG. 2007. Systemic
634 inactivation and phenotypic characterization of two-component systems in expression
635 of *Streptococcus mutans* virulence properties. *Lett Appl Microbiol* 45:398-404.

636 28. Okinaga T, Xie Z, Niu G, Qi F, Merritt J. 2010. Examination of the *hdrRM* regulon
637 yields insight into the competence system of *Streptococcus mutans*. *Mol Oral Microbiol*
638 25:165-177.

639 29. Qi F, Merritt J, Lux R, Shi W. 2004. Inactivation of the ciaH Gene in *Streptococcus*
640 *mutans* diminishes mutacin production and competence development, alters sucrose-
641 dependent biofilm formation, and reduces stress tolerance. *Infect Immun* 72:4895-4899.

642 30. Underhill SAM, Shields RC, Burne RA, Hagen SJ. 2019. Carbohydrate and PepO
643 control bimodality in competence development by *Streptococcus mutans*. *Mol*
644 *Microbiol* 112:1388-1402.

645 31. Xie Z, Okinaga T, Niu G, Qi F, Merritt J. 2010. Identification of a novel bacteriocin
646 regulatory system in *Streptococcus mutans*. *Mol Microbiol* 78:1431-1447.

647 32. Chastanet A, Prudhomme M, Claverys JP, Msadek T. 2001. Regulation of
648 *Streptococcus pneumoniae clp* genes and their role in competence development and
649 stress survival. *J Bacteriol* 183:7295-7307.

650 33. Shields RC, Zeng L, Culp DJ, Burne RA. 2018. Genomewide Identification of Essential
651 Genes and Fitness Determinants of *Streptococcus mutans* UA159. *mSphere* 3:e00031-
652 18.

653 34. Cui L, Vigouroux A, Rousset F, Varet H, Khanna V, Bikard D. 2018. A CRISPRi screen
654 in *E. coli* reveals sequence-specific toxicity of dCas9. *Nat Commun* 9:1912.

655 35. Liu X, Gallay C, Kjos M, Domenech A, Slager J, van Kessel SP, Knoops K, Sorg RA,
656 Zhang JR, Veening JW. 2017. High-throughput CRISPRi phenotyping identifies new
657 essential genes in *Streptococcus pneumoniae*. *Mol Syst Biol* 13:931.

658 36. Liu X, Kimmey JM, Matarazzo L, de B, V, Van ML, Sirard JC, Nizet V, Veening JW.
659 2021. Exploration of bacterial bottlenecks and *Streptococcus pneumoniae* pathogenesis
660 by CRISPRi-Seq. *Cell Host Microbe* 29:107-120.

661 37. Van den Bogert B, Boekhorst J, Herrmann R, Smid EJ, Zoetendal EG, Kleerebezem M.
662 2013. Comparative genomics analysis of Streptococcus isolates from the human small
663 intestine reveals their adaptation to a highly dynamic ecosystem. *PLoS One* 8:e83418.

664 38. Sorg RA, Kuipers OP, Veening JW. 2015. Gene expression platform for synthetic
665 biology in the human pathogen *Streptococcus pneumoniae*. *ACS Synth Biol* 4:228-239.

39. Boutry C, Wahl A, Delplace B, Clippe A, Fontaine L, Hols P. 2012. Adaptor protein MecA is a negative regulator of the expression of late competence genes in *Streptococcus thermophilus*. *J Bacteriol* 194:1777-1788.

40. Knoops A, Ledesma-Garcia L, Waegemans A, Lamontagne M, Decat B, Degand H, Morsomme P, Soumillion P, Delvigne F, Hols P. 2022. Competence shut-off by intracellular pheromone degradation in salivarius streptococci. *PLoS Genet* 18:e1010198.

41. Li W, Koster J, Xu H, Chen CH, Xiao T, Liu JS, Brown M, Liu XS. 2015. Quality control, modeling, and visualization of CRISPR screens with MAGeCK-VISPR. *Genome Biol* 16:281.

42. Wahl A, Servais F, Drucbert AS, Foulon C, Fontaine L, Hols P. 2014. Control of natural transformation in salivarius Streptococci through specific degradation of sigmaX by the MecA-ClpCP protease complex. *J Bacteriol* 196:2807-2816.

43. Claverys JP, Havarstein LS. 2007. Cannibalism and fratricide: mechanisms and raisons d'etre. *Nat Rev Microbiol* 5:219-229.

44. Tatusov RL, Galperin MY, Natale DA, Koonin EV. 2000. The COG database: a tool for genome-scale analysis of protein functions and evolution. *Nucleic Acids Res* 28:33-36.

45. Neuhaus FC, Baddiley J. 2003. A continuum of anionic charge: structures and functions of D-alanyl-teichoic acids in gram-positive bacteria. *Microbiol Mol Biol Rev* 67:686-723.

46. Levander F, Radstrom P. 2001. Requirement for phosphoglucomutase in exopolysaccharide biosynthesis in glucose- and lactose-utilizing *Streptococcus thermophilus*. *Appl Environ Microbiol* 67:2734-2738.

47. Henry C, Haller L, Blein-Nicolas M, Zivy M, Canette A, Verbrugghe M, Mezange C, Boulay M, Gardan R, Samson S, Martin V, Andre-Leroux G, Monnet V. 2019. Identification of Hanks-Type Kinase PknB-Specific Targets in the *Streptococcus thermophilus* Phosphoproteome. *Front Microbiol* 10:1329.

48. Pereira SF, Goss L, Dworkin J. 2011. Eukaryote-like serine/threonine kinases and phosphatases in bacteria. *Microbiol Mol Biol Rev* 75:192-212.

49. Devine KM. 2018. Activation of the PhoPR-Mediated Response to Phosphate Limitation Is Regulated by Wall Teichoic Acid Metabolism in *Bacillus subtilis*. *Front Microbiol* 9:2678.

50. Eldholm V, Gutt B, Johnsborg O, Bruckner R, Maurer P, Hakenbeck R, Mascher T, Havarstein LS. 2010. The pneumococcal cell envelope stress-sensing system LiaFSR is activated by murein hydrolases and lipid II-interacting antibiotics. *J Bacteriol* 192:1761-1773.

51. Ganguly T, Kajfasz JK, Abranches J, Lemos JA. 2020. Regulatory circuits controlling Spx levels in *Streptococcus mutans*. *Mol Microbiol* 114:109-126.

52. Rojas-Tapias DF, Helmann JD. 2018. Stabilization of *Bacillus subtilis* Spx under cell wall stress requires the anti-adaptor protein YirB. *PLoS Genet* 14:e1007531.

53. Suntharalingam P, Senadheera MD, Mair RW, Levesque CM, Cvitkovitch DG. 2009. The LiaFSR system regulates the cell envelope stress response in *Streptococcus mutans*. *J Bacteriol* 191:2973-2984.

54. Ulrych A, Fabrik I, Kupcik R, Vajrychova M, Doubravova L, Branny P. 2021. Cell Wall Stress Stimulates the Activity of the Protein Kinase StkP of *Streptococcus pneumoniae*, Leading to Multiple Phosphorylation. *J Mol Biol* 433:167319.

55. Shah IM, Laaberki MH, Popham DL, Dworkin J. 2008. A eukaryotic-like Ser/Thr kinase signals bacteria to exit dormancy in response to peptidoglycan fragments. *Cell* 135:486-496.

56. Beilharz K, Novakova L, Fadda D, Branny P, Massidda O, Veening JW. 2012. Control of cell division in *Streptococcus pneumoniae* by the conserved Ser/Thr protein kinase StkP. *Proc Natl Acad Sci U S A* 109:E905-E913.

57. Dias R, Felix D, Canica M, Trombe MC. 2009. The highly conserved serine threonine kinase StkP of *Streptococcus pneumoniae* contributes to penicillin susceptibility independently from genes encoding penicillin-binding proteins. *BMC Microbiol* 9:121.

58. Fleurie A, Cluzel C, Guiral S, Freton C, Galisson F, Zanella-Cleon I, Di Guilmi AM, Grangeasse C. 2012. Mutational dissection of the S/T-kinase StkP reveals crucial roles in cell division of *Streptococcus pneumoniae*. *Mol Microbiol* 83:746-758.

59. Zhang R, Xu W, Shao S, Wang Q. 2021. Gene Silencing Through CRISPR Interference in Bacteria: Current Advances and Future Prospects. *Front Microbiol* 12:635227.

60. Tian XL, Dong G, Liu T, Gomez ZA, Wahl A, Hols P, Li YH. 2013. MecA protein acts as a negative regulator of genetic competence in *Streptococcus mutans*. *J Bacteriol* 195:5196-5206.

61. Shields RC, O'Brien G, Maricic N, Kesterson A, Grace M, Hagen SJ, Burne RA. 2018. Genome-Wide Screens Reveal New Gene Products That Influence Genetic Competence in *Streptococcus mutans*. *J Bacteriol* 200:e00508-17.

62. Dmitriev A, Mohapatra SS, Chong P, Neely M, Biswas S, Biswas I. 2011. CovR-controlled global regulation of gene expression in *Streptococcus mutans*. *PLoS One* 6:e20127.

63. Stevens KE, Chang D, Zwack EE, Sebert ME. 2011. Competence in *Streptococcus pneumoniae* is regulated by the rate of ribosomal decoding errors. *mBio* 2:e00071-11.

64. Khemici V, Prudhomme M, Polard P. 2021. Tight Interplay between Replication Stress and Competence Induction in *Streptococcus pneumoniae*. *Cells* 10:1938.

65. Slager J, Kjos M, Attaiech L, Veening JW. 2014. Antibiotic-induced replication stress triggers bacterial competence by increasing gene dosage near the origin. *Cell* 157:395-406.

743 66. Winther KS, Roghanian M, Gerdes K. 2018. Activation of the Stringent Response by
744 Loading of RelA-tRNA Complexes at the Ribosomal A-Site. *Mol Cell* 70:95-105.

745 67. Kaspar J, Kim JN, Ahn SJ, Burne RA. 2016. An Essential Role for (p)ppGpp in the
746 Integration of Stress Tolerance, Peptide Signaling, and Competence Development in
747 *Streptococcus mutans*. *Front Microbiol* 7:1162.

748 68. Horstmann N, Saldana M, Sahasrabhojane P, Yao H, Su X, Thompson E, Koller A,
749 Shelburne SA, III. 2014. Dual-site phosphorylation of the control of virulence regulator
750 impacts group a streptococcal global gene expression and pathogenesis. *PLoS Pathog*
751 10:e1004088.

752 69. Lin WJ, Walthers D, Connelly JE, Burnside K, Jewell KA, Kenney LJ, Rajagopal L.
753 2009. Threonine phosphorylation prevents promoter DNA binding of the Group B
754 Streptococcus response regulator CovR. *Mol Microbiol* 71:1477-1495.

755 70. Dufour D, Villemin C, Perry JA, Levesque CM. 2016. Escape from the competence
756 state in *Streptococcus mutans* is governed by the bacterial population density. *Mol Oral*
757 *Microbiol* 31:501-514.

758 71. Mignolet J, Fontaine L, Kleerebezem M, Hols P. 2016. Complete Genome Sequence of
759 *Streptococcus salivarius* HSISS4, a Human Commensal Bacterium Highly Prevalent in
760 the Digestive Tract. *Genome Announc* 4:e01637-15.

761 72. Letort C, Juillard V. 2001. Development of a minimal chemically-defined medium for
762 the exponential growth of *Streptococcus thermophilus*. *J Appl Microbiol* 91:1023-1029.

763 73. Fontaine L, Dandoy D, Boutry C, Delplace B, de Frahan MH, Fremaux C, Horvath P,
764 Boyaval P, Hols P. 2010. Development of a versatile procedure based on natural
765 transformation for marker-free targeted genetic modification in *Streptococcus*
766 *thermophilus*. *Appl Environ Microbiol* 76:7870-7877.

767 74. Dorrazehi GM, Worms S, Chirakadavil JB, Mignolet J, Hols P, Soumillion S. 2020.
768 Building Scarless Gene Libraries in the Chromosome of Bacteria, p 189-211. *In*: Iranzo
769 O, Roque A (ed), Peptide and Protein Engineering, Springer Protocols Handbooks.
770 Humana, New York, NY.

771 75. Lu S, Wang J, Chitsaz F, Derbyshire MK, Geer RC, Gonzales NR, Gwadz M, Hurwitz
772 DI, Marchler GH, Song JS, Thanki N, Yamashita RA, Yang M, Zhang D, Zheng C,
773 Lanczycki CJ, Marchler-Bauer A. 2020. CDD/SPARCLE: the conserved domain
774 database in 2020. *Nucleic Acids Res* 48:D265-D268.

775 76. Ogura M, Hashimoto H, Tanaka T. 2002. Med, a cell-surface localized protein
776 regulating a competence transcription factor gene, *comK*, in *Bacillus subtilis*. *Biosci*
777 *Biotechnol Biochem* 66:892-896.
778
779

780

TABLES AND FIGURES

Table 1. gRNA identification in spontaneous transformants

gRNA ID	Genome position	Interference target	Gene name	Locus tag	Comment/function	Transformation rate
g_37	83910	Gene	*clpC*	HSISS4_00061	ComX degradation machinery ClpC	2.00E-06
g_38	85320	Gene	*clpC*	HSISS4_00061	ComX degradation machinery ClpC	6.00E-06
g_39	412742	Gene	*pepF*	HSISS4_00369	Oligoendopeptidase F	4.00E-06
g_27	1589000	Gene		HSISS4_01391	Bactoprenol glucosyltransferase	3.40E-02
g_30	1823312	Gene		HSISS4_01622	Hypothetical protein	2.00E-06
g_32	875880	Gene		HSISS4_00805	Hypothetical protein	5.80E-04
g_35	1442100	Gene		HSISS4_01302	Hypothetical protein	4.00E-06
g_33	multiple sites	Ribosomal RNA			16S ribosomal RNA	4.00E-06
g_34	multiple sites	Ribosomal RNA			16S ribosomal RNA	2.00E-06
g_36	multiple sites	Ribosomal RNA			16S ribosomal RNA	2.00E-06
g_26	112760	Gene	*gpmB*	HSISS4_00092	Phosphoglycerate mutase	ND[a]
g_42	499523	Gene	*carB*	HSISS4_00444	Carbamoyl synthase	ND
g_40 [b]	1270227	Gene	*scuR*	HSISS4_01166	Intracellular receptor, bacteriocin-related communication system	ND
g_40 [b]	1272924	Gene	*sarF*	HSISS4_01169	Intracellular receptor, bacteriocin-related communication system	ND
g_41	1775841	Gene	*pepXP*	HSISS4_01580	Dipeptidyl peptidase	ND
g_31	714120	Gene		HSISS4_00663	Extracellular nuclease 2	ND
g_43	664598	Intergenic				ND

[a] ND, not detected.

[b] g_40 gRNA recognizes both *scuR* and *sarF* genes.

786 **Table 2. Identification of competence costly genes from the gRNA depletion screen**

Gene name	Locus tag	Comment/function	Fitness cost score without competence induction [a]	Std residual (< -2.5) [b]
Competence-related				
comR	HSISS4_00217	Competence intracellular receptor	0.00	-5.58
amiF1	HSISS4_01361	Oligopeptide ABC transporter, ATP-binding subunit F	-0.52	-2.94
amiE	HSISS4_01362	Oligopeptide ABC transporter, ATP-binding subunit E	-0.47	-3.68
amiD	HSISS4_01363	Oligopeptide ABC transporter, permease subunit D	-0.52	-3.53
amiC	HSISS4_01364	Oligopeptide ABC transporter, permease subunit C	-0.51	-3.59
amiA3A	HSISS4_01365	Oligopeptide ABC transporter, oligopeptide binding subunit A	-0.44	-3.37
	HSISS4_01664	SlvX immunity protein	0.08	-4.94
slvX	HSISS4_01665	Bacteriocin	-0.04	-4.73
mecA	HSISS4_00128	ComX degradation machinery adaptor protein	-0.22	-6.19
spxA1	HSISS4_00943	Transcriptional regulator	0.38	-2.80
Cell-envelope-related				
stkP	HSISS4_01348	Serine-Threonine kinase	0.44	-2.98
acpP1	HSISS4_00021	Acyl carrier protein	0.06	-2.54
rgpG	HSISS4_00129	Polysaccharide synthesis protein	-0.21	-5.92
rgpF	HSISS4_01378	Polysaccharide synthesis protein	-0.21	-4.43
rgpE	HSISS4_01379	Extracellular rhamnan synthesis protein	-0.94	-5.20
rgpA2	HSISS4_01383	Extracellular rhamnan synthesis protein	-2.37	-3.52
rmlA1	HSISS4_00723	Rhamnose synthesis protein	-0.55	-6.66
rmlC	HSISS4_00724	Rhamnose synthesis protein	-0.69	-4.77
rmlB	HSISS4_00725	Rhamnose synthesis protein	-0.85	-4.62
pgmA	HSISS4_01102	Phosphoglucomutase	-0.12	-3.61
dgk	HSISS4_00536	Lipid carrier recycler	-2.28	-2.71
murG	HSISS4_00684	Peptidoglycan Lipid II precursor synthesis	-3.98	-2.62
	HSISS4_00889	Exporter of O-antigen, teichoic acids, lipoteichoic acids (WpsG)	-0.24	-3.97
dltD	HSISS4_01108	Poly(glycerolphosphate chain) D-alanine transfer protein	-0.03	-2.98
dltC	HSISS4_01109	D-Alanine phosphoribitol ligase subunit 2	-0.48	-3.68
dltB	HSISS4_01110	D-alanyl transfer protein	-0.31	-3.87
dltA	HSISS4_01111	D-Alanine phosphoribitol ligase subunit 1	-0.39	-3.52
dltX	HSISS4_01112	D-Ala-teichoic acid biosynthesis protein	-0.63	-2.93
pstB1	HSISS4_00936	Phosphate transport, ATP binding protein	0.37	-3.00
pstC2	HSISS4_00937	Phosphate transport, permease protein	0.38	-3.39
pstC1	HSISS4_00938	Phosphate transport, permease protein	0.38	-3.27
pstS	HSISS4_00939	Phosphate transport, phosphate binding protein	0.40	-3.14
divIC	HSISS4_00008	Cell division protein	-3.85	-5.27

ftsL	HSISS4_01598	Cell division protein	-4.12	-3.29
Translation				
prfB	HSISS4_00848	Peptide chain release factor	-0.06	-4.39
proS	HSISS4_00152	Prolyl tRNA synthetase	-3.77	-2.53
rplM	HSISS4_00076	Large subunit ribosomal protein	-3.67	-3.53
rplX	HSISS4_01812	Large subunit ribosomal protein	-3.51	-4.15
rpsU	HSISS4_01396	Small subunit ribosomal protein	-1.23	-5.40
rpsF	HSISS4_01661	Small subunit ribosomal protein	-3.81	-3.04
rpsE	HSISS4_01806	Small subunit ribosomal protein	-3.88	-2.64
rpsS	HSISS4_01819	Small subunit ribosomal protein	-3.84	-2.90
	HSISS4_00271	Ribosomal protein	-3.75	-2.80
	HSISS4_r00031	tRNA Met	-4.37	-7.16
	HSISS4_r00059	tRNA Glu	-4.03	-3.17
	HSISS4_r00070	tRNA Arg	-3.67	-2.56
Others				
ctsR	HSISS4_00060	Stress transcriptional regulator	-0.09	-2.57
atpE	HSISS4_00399	ATP synthase	-3.15	-2.65
pyrH	HSISS4_00354	Uridine monophosphate kinase	-0.94	-3.03
sipA	HSISS4_01673	Secretory signal peptidase	-0.87	-2.63
	HSISS4_00898	Permease	0.05	-2.73
	HSISS4_00523	Hypothetical protein	0.16	-3.82
	HSISS4_00888	Hypothetical protein	-0.03	-3.30

[a] Fitness-cost scores were computed with the MAGeCK algorithm (41) by comparing the total depletion of gRNAs per gene in the mock condition with the library-induced condition (Ci).
[b] Standardized (Std) residuals (cut-off value < -2.5) were calculated as the deviation from the linear regression performed with the fitness-cost scores for conditions with library induction (Ci) and with library induction together with competence induction (Ci+C).

793 **Table 3. Identification of competence-associated antagonist genes from β-Gal screen**

Gene name	Locus tag	Comment/function	Normalized count (> 0.01) [a]	Mean log2(FC) Lux (> 0.5) [b]
Competence-related [c]				
hk13	HSISS4_01230	Histidine kinase	0.03	1.80
manL1	HSISS4_00257	PTS system, mannose-specific IIAB component	0.34	0.66
manM1	HSISS4_00256	PTS system, mannose-specific IIC component	0.17	0.66
manN1	HSISS4_00255	PTS system, mannose-specific IID component	0.19	0.70
med	HSISS4_01089	Nucleoside-binding protein	0.06	0.57
Cell-enveloppe-related				
stkP	HSISS4_01348	Serine-threonine protein kinase	0.10	1.02
LiaF	HSISS4_01346	LiaSR-associated transporter	0.04	1.08
plsX	HSISS4_00020	Phosphate:acyl-ACP acyltransferase	0.11	1.52
	HSISS4_01826	Acyltransferase family	0.04	0.72
murJ	HSISS4_00717	Lipid II flippase	0.06	1.28
murC	HSISS4_00190	UDP-N-acetylmuramate-alanine ligase	0.04	0.81
murZ	HSISS4_01465	UDP-N-acetylglucosamine 1-carboxyvyniltransferase	0.03	1.41
glmS	HSISS4_01060	Glucosamine--fructose-6-phosphate aminotransferase isomerizing	0.02	0.80
gcaD	HSISS4_00481	N-acetylglucosamine-1-phosphate uridyltransferase/Glucosamine-1-phosphate N-acetyltransferase (GlmU)	0.02	0.86
rgpX3	HSISS4_01386	Heteropolysaccharide repeat unit export protein	0.04	1.44
	HSISS4_00330	Lipopolysaccharide biosynthesis protein	0.04	0.85
dltA	HSISS4_01111	D-alanine--poly(phosphoribitol) ligase subunit 1	0.04	0.67
dltB	HSISS4_01110	D-alanyl transfer protein	0.02	1.17
pstC1	HSISS4_00938	Phosphate transport system permease protein	0.03	1.29
pgmA	HSISS4_01102	Phosphoglucomutase	0.05	0.98
asp3	HSISS4_01316	Accessory secretory protein	0.04	0.71
pcsB2	HSISS4_00358	GBS surface immunogenic protein	0.02	1.48
Amino-acid metabolism				
sdaA	HSISS4_01162	L-serine dehydratase, alpha subunit	0.05	1.26
argJ	HSISS4_00385	Glutamate N-acetyltransferase/N-acetylglutamate synthase	0.02	0.98
pepP	HSISS4_01648	Aminopeptidase P	0.06	1.10
pepS	HSISS4_00051	Aminopeptidase S	0.02	0.73
gnlP	HSISS4_01405	Glutamine ABC transporter/ glutamine-binding permease	0.04	0.77
livG2	HSISS4_00477	ABC-type multidrug transport transport system, ATPase component	0.06	0.60
livJ	HSISS4_00287	High-affinity leucine-specific transport system	0.03	1.38
	HSISS4_00832	Glutamate transport membrane-spanning protein	0.03	1.26
	HSISS4_00833	Glutamate transport permease protein	0.05	1.10
Others				
galR	HSISS4_01243	Galactose operon repressor	0.03	0.68
	HSISS4_01867	Transcriptional regulator, PadR family	0.08	1.02
nusA	HSISS4_00269	Transcription termination protein	0.03	1.66

cshA	HSISS4_01831	Chromosome segregation helicase	0.03	0.56
	HSISS4_00847	Epoxyqueuosine (oQ) reductase	0.02	0.69
gidA	HSISS4_01879	tRNA uridine 5-carboxymethylaminomethyl modification enzyme	0.02	0.79
	HSISS4_01426	Acetyltransferase	0.07	0.97
	HSISS4_01531	RNA binding protein	0.08	0.79
trxA1A	HSISS4_00080	Thioredoxin	0.13	0.76
dnaK1	HSISS4_00097	Chaperone protein	0.02	1.77
scrK	HSISS4_01640	Fructokinase	0.10	0.87
tpiA	HSISS4_00409	Triosephosphate isomerase	0.08	0.85
purF	HSISS4_00024	Amidophosphoribosyltransferase	0.02	0.76
pyrDb	HSISS4_00974	Dihydroorotate dehydrogenase, catalytic subunit	0.02	1.13
	HSISS4_01010	Phenazine biosynthesis-like protein	0.13	0.75
	HSISS4_00044	hypothetical protein	0.25	0.95
	HSISS4_00614	hypothetical protein	0.03	0.92
	HSISS4_01307	hypothetical protein	0.03	0.95

[a] Normalized counts (cut-off value > 0.01) were calculated by dividing the number of gRNAs targeting one gene by the expected number of gRNAs targeting this gene in the library.

[b] Mean of the $\log_2$ fold-change is an average of all the fold-changes in specific Lux activity for the different gRNAs targeting the same gene (cut-off value > 0.5).

[c] *hk13*, *manLMN*, *med* genes were previously reported as involved in competence regulation in *S. salivarius*, *S. mutans*, and *B. subtilis* respectively (7, 30, 76).

802

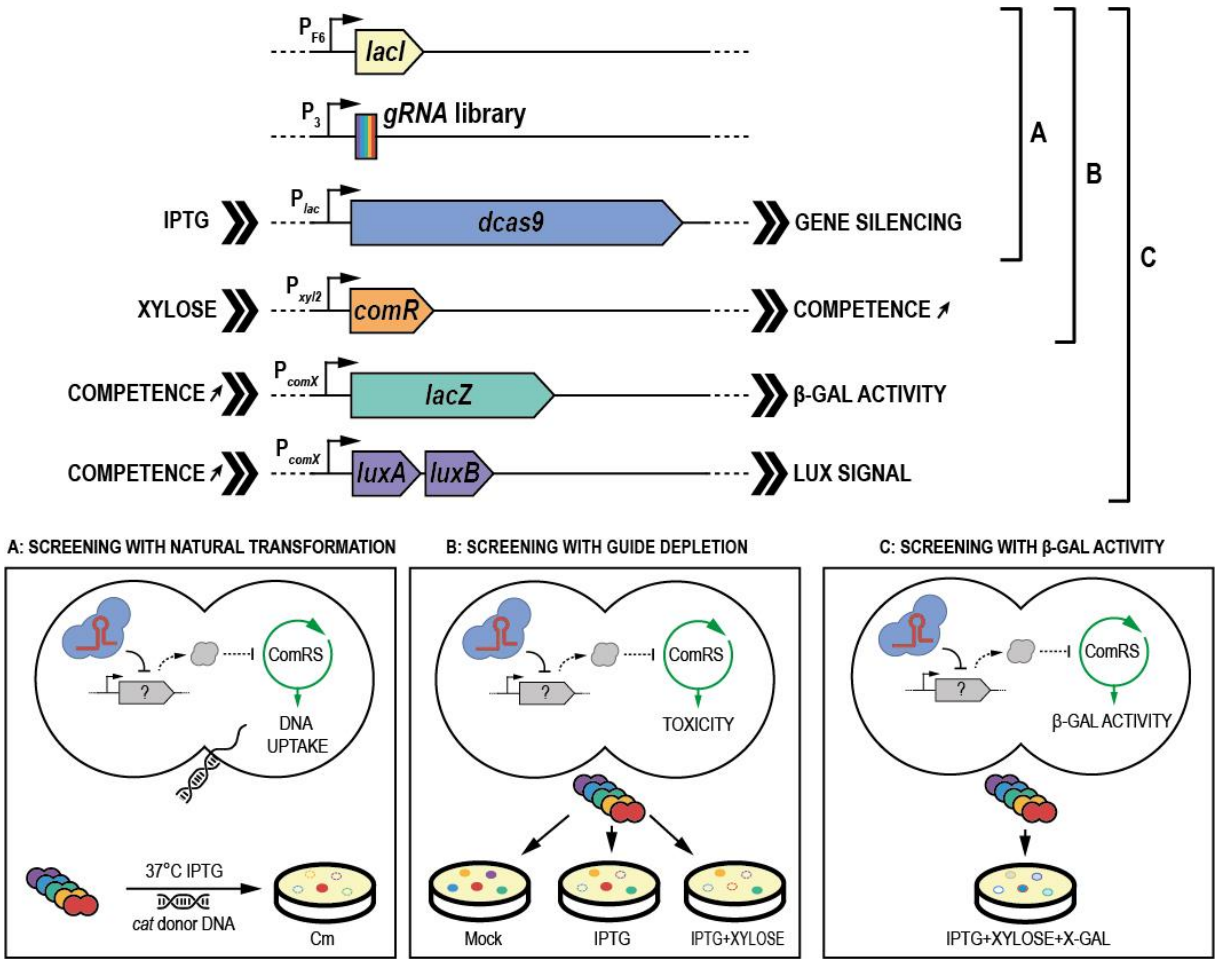

803

804 **Figure 1. CRISPRi screening strategies for competence modulators in *S. salivarius.*** A
805 library of gRNAs was designed and introduced (P_3-*gRNA*) in an engineered strain of *S.*
806 *salivarius* harboring an IPTG-inducible system for dCas9 (P_{F6}-*lacI*; P_{lac}-*dcas9*). A first library
807 was screened for spontaneous competence activation upon dCas9-inhibition by growing cells
808 in chemically defined medium in presence of IPTG and *cat* donnor DNA. The selection on
809 chloramphenicol plates was associated with inhibition of competence negative players (**A**). A
810 second library was generated by introducing the gRNA library into the same background with
811 a supplemental construct consisting of a xylose-inducible promoter fused to *comR* (P_{xyl2}-*comR*).
812 The library was spread on control (mock), gRNA library-induced (IPTG) or gRNA library- and
813 competence-induced (IPTG + xylose) plates. NGS analysis of depleted gRNAs in the three
814 conditions was performed to search for costly genes only associated to competence (**B**). A third
815 library was built by adding *lacZ* under the control of P_{comX} (P_{comX}-*lacZ*) together with a
816 competence luciferase reporter system (P_{comX}-*luxAB*) to the previous strain and transferring the
817 gRNA library into this background. The generated library was screened on plates containing
818 IPTG, xylose and X-gal. gRNAs targeting potential competence inhibitory or activatory genes
819 were associated to dark blue or white phenotypes, respectively (**C**).

820

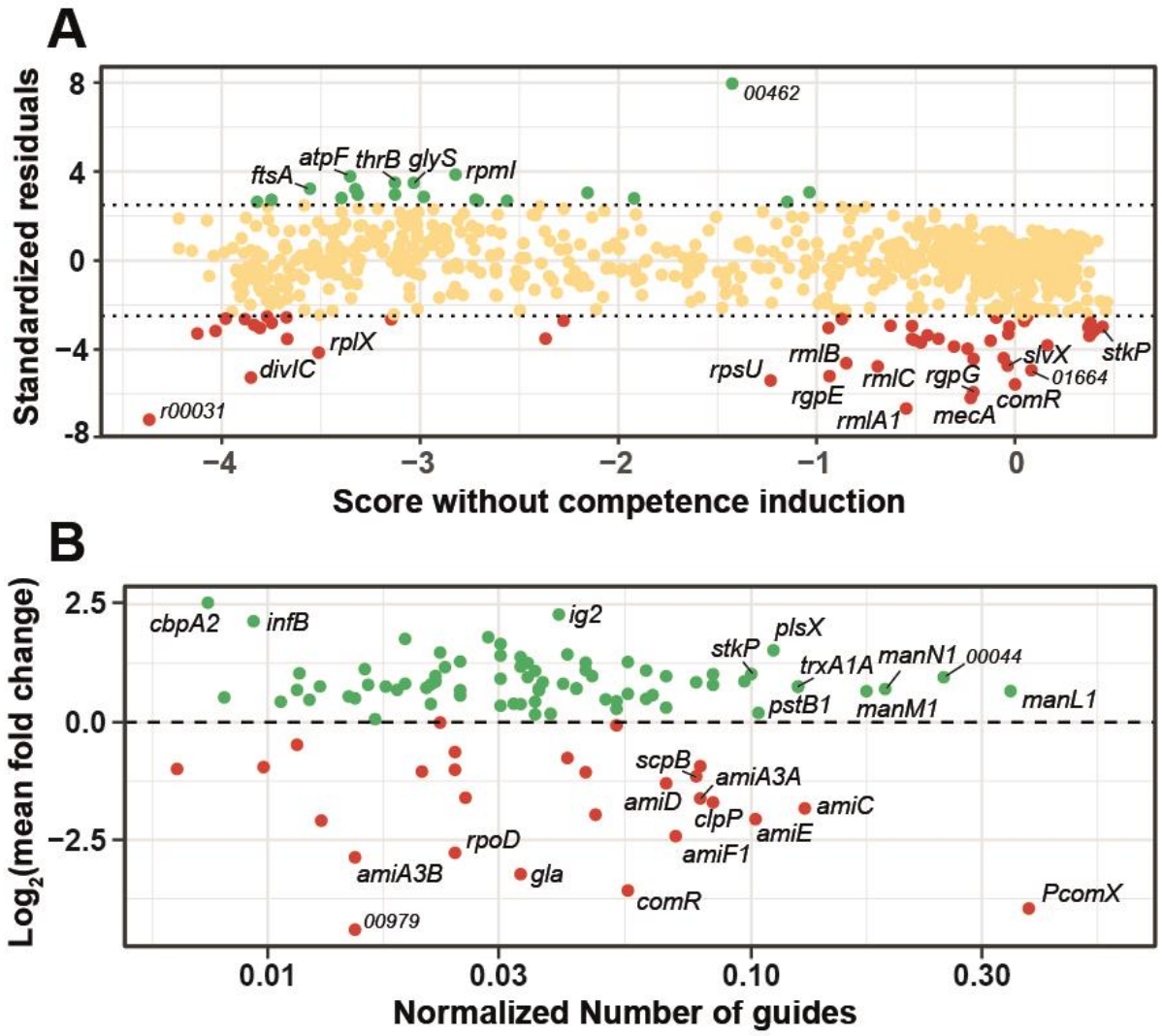

Figure 2. Selection of genes from CRISPRi screens. A. gRNA depletion screen. The gRNA library was grown on M17G plates for ~ 12 generations with no induction (mock), with gRNA library induction (Ci), or with gRNA library and competence induction (Ci+C). The gRNAs (4 technical replicates per condition, ~40 M reads) were sequenced and mapped thanks to the MAGeCK-VISPR algorithm (41). Using the same tool, we identify gRNA depletion in costly genes linked to library induction only (Ci vs mock) and both library and competence induction (Ci vs Ci+C) (Fig. S2). We then compared the gRNA depletion scores for each gene in both induction systems and performed a linear regression (Fig. S3). Standardized residuals of the regression were then computed and plotted in function of the score of each gene in the condition without competence induction (Ci). Positive (green) and negative (red) standardized residuals (arbitrary cut-off of +2.5 and -2.5) denote genes with enriched or depleted gRNAs, respectively. Dots in yellow are considered as non-significantly affected genes. **B.** β-Gal screen. After library production (~10^5 colonies), screening for dark blue and white clones on M17GL plates (with IPTG, xylose, and X-gal; P_{comX}-*lacZ*, P_{xyl2}-*comR*) and validation with luciferase assays (P_{comX}-*luxAB*), clones with the most dissimilar luciferase phenotypes (141 dark blue and 68 white clones) were sequenced for gRNA identification. The y-axis displays the mean fold change Log_2 value of luciferase activity calculated on all the gRNAs targeting the same gene. The x-axis displays the number of gRNAs targeting the same gene normalized by the expected total

number of gRNAs present in the library for this gene. Green dots and red dots denote gene inhibition resulting in competence overactivation or repression, respectively.

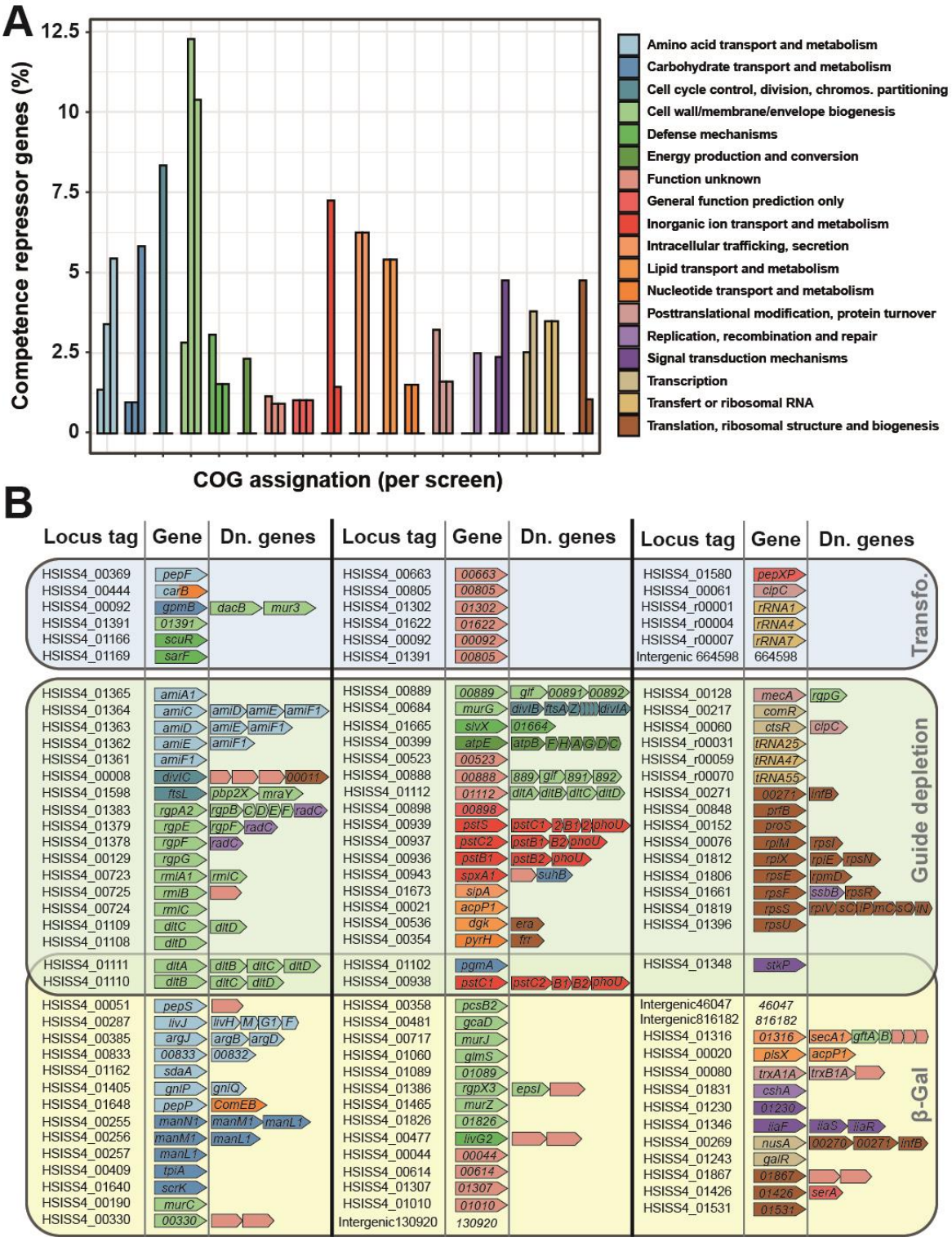

Figure 3. Functional assignation of competence repressor genes from CRISPRi screens. **A.** Relative abundance of COG-assigned genes. A COG assignation was associated to every gene from the HSISS4 genome. For each COG type, the proportion (%) of selected genes with a defined screen was calculated against all the genes with this COG assignation of the genome. This proportion is displayed per screen (1st bar, transformation screen; 2nd bar, gRNA depletion screen; 3rd bar, β-Gal screen). **B.** Details of all selected genes displayed per screen. Operons (Dn. genes) are shown since CRISPRi also silences downstream genes. Genes are colored according to their COG assignation.

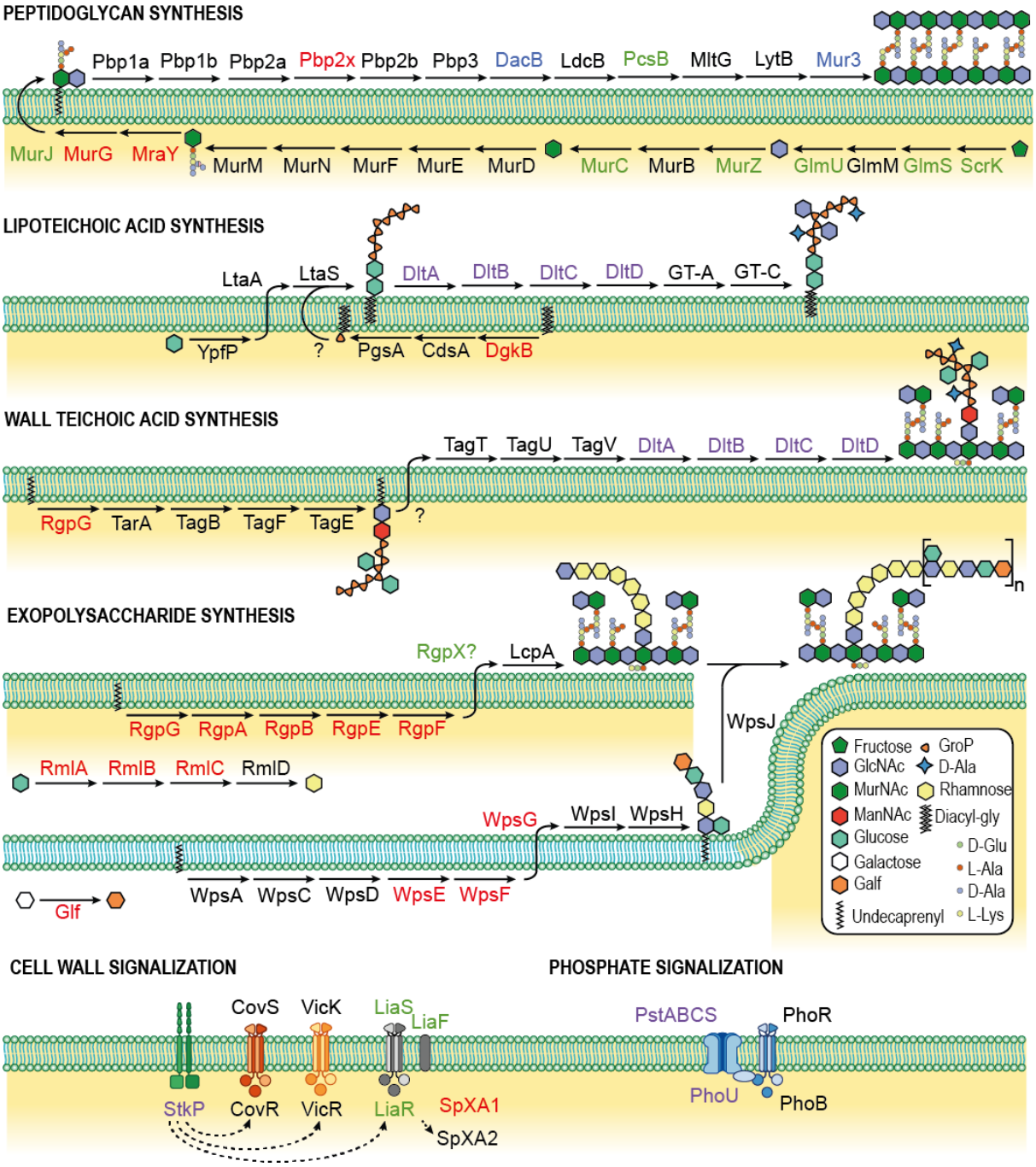

Figure 4. Cell-wall pathways and competence negative modulators from CRISPRi screens. Major cell-wall biosynthesis and signalization pathways are depicted. Proteins selected by the transformation, gRNA depletion, and β-gal screens are shown in blue, red, and green, respectively. Proteins selected in both gRNA depletion and β-gal screens are shown in light violet. In the absence of literature for complete reconstructed pathways, lipoteichoic acid synthesis is based on knowledge from *Staphylococcus aureus*, wall teichoic acid from *B. subtilis* 168 and polysaccharide synthesis from *L. lactis*. HSISS4_00889, 00890, 00891 and 00892 were renamed with *Lactococcus lactis* homologs WpsG, Glf, WpsE and WpsF, respectively. GlcNAc, *N*-acetylglucosamine; MurNAc, *N*-acetyl muramic acid; ManNAc, *N*-acetylmannosamine; Galf, Galactofuranose; Diacyl-gly, Diacyl-glycerol; GroP, Glycerol-phosphate.

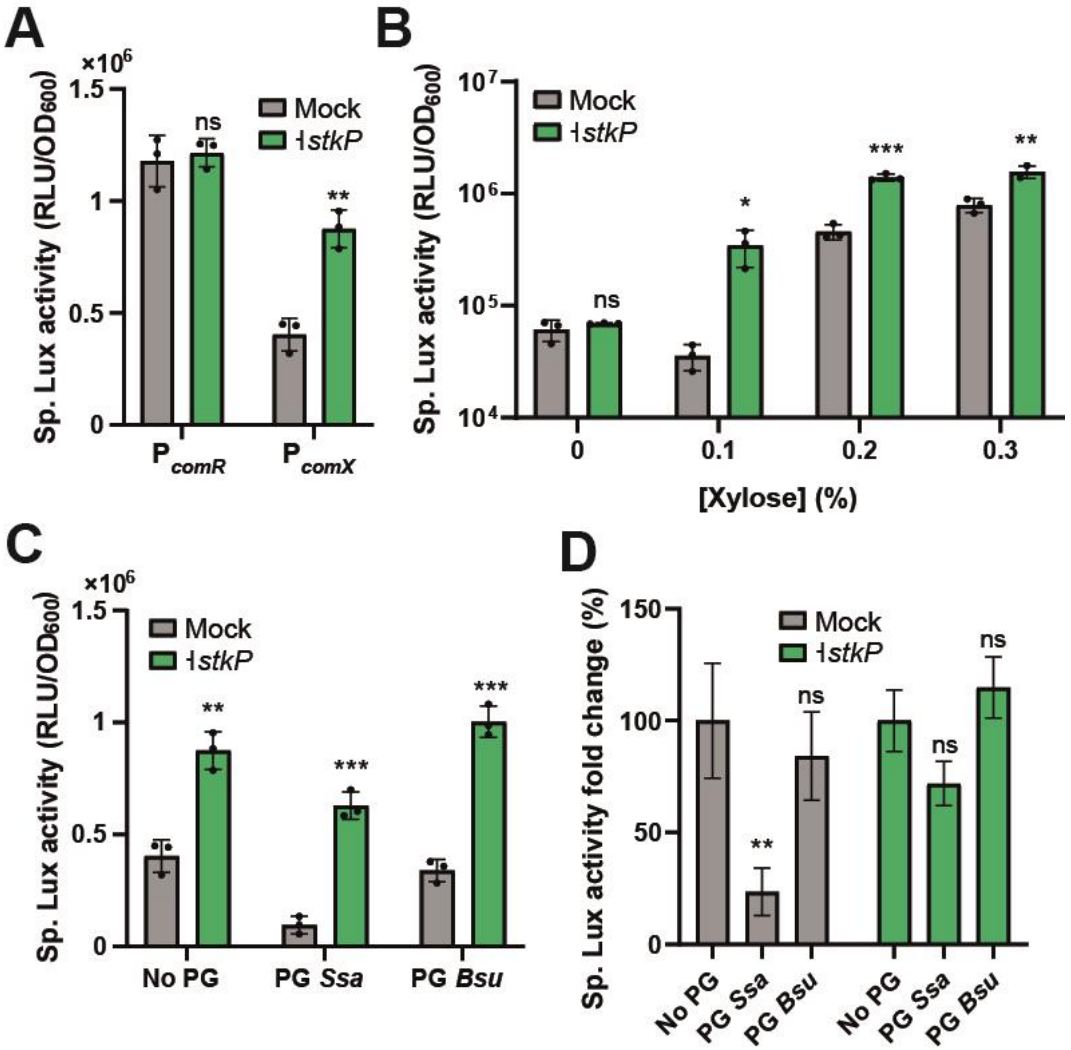

Figure 5. StkP controls *comX* expression by sensing peptidoglycan extracts. A. Effect of *stkP* inhibition on *comR* and *comX* expression. A dCas9 module (P_{F6}-*lacI*; P_{lac}-*dcas9*) together with a gRNA targeting *stkP* (P_3-*g_23*) were used to inhibit *stkP* transcription. The dCas9 interference system was associated to a P_{comR}-*luxAB* or a P_{comX}-*luxAB* reporter fusion together with a xylose-inducible *comR* module (P_{xyl2}-*comR*). Mock denotes the same strain without dCas9 interference. **B.** Effect of ComR level on StkP-mediated activation of *comX*. The P_{comX}-*luxAB* P_{xyl2}-*comR* strain (described in A) was incubated with various xylose concentrations (0, 0.1, 0.2, 0.3%) with or without *stkP* inhibition. **C.** Effect of peptidoglycan (PG) extracts on StkP-mediated activation of *comX*. PG extracts of *S. salivarius* (PG *Ssa*) or *B. subtilis* (PG *Bsu*) were added to a culture of the P_{comX}-*luxAB* strain (described in A) at a final concentration of 0.3 mg/ml. **D.** Specific Lux activity (%) calculated between the culture with no addition of PG extracts (No PG, 100%) and the related condition. Percentages were calculated with the data presented in C. For P_{comX}-*luxAB* activation, xylose 0.25% was used except if else stated. For CRISPRi *stkP* inhibition, IPTG 1 mM was used. Dots denote technical triplicate values for mock and biological triplicate values for mutants, ± standard deviation. Statistical *t*-test was performed for each condition in comparison to related control (Ctrl: mock; panels A, B, and D) or one-way ANOVA with Dunett's test for multiple comparison (Ctrl: No PG; panel E). ns, non-significative; $P > 0.05$; *, $P < 0.05$; **, $P < 0.01$; ***, $P < 0.001$.

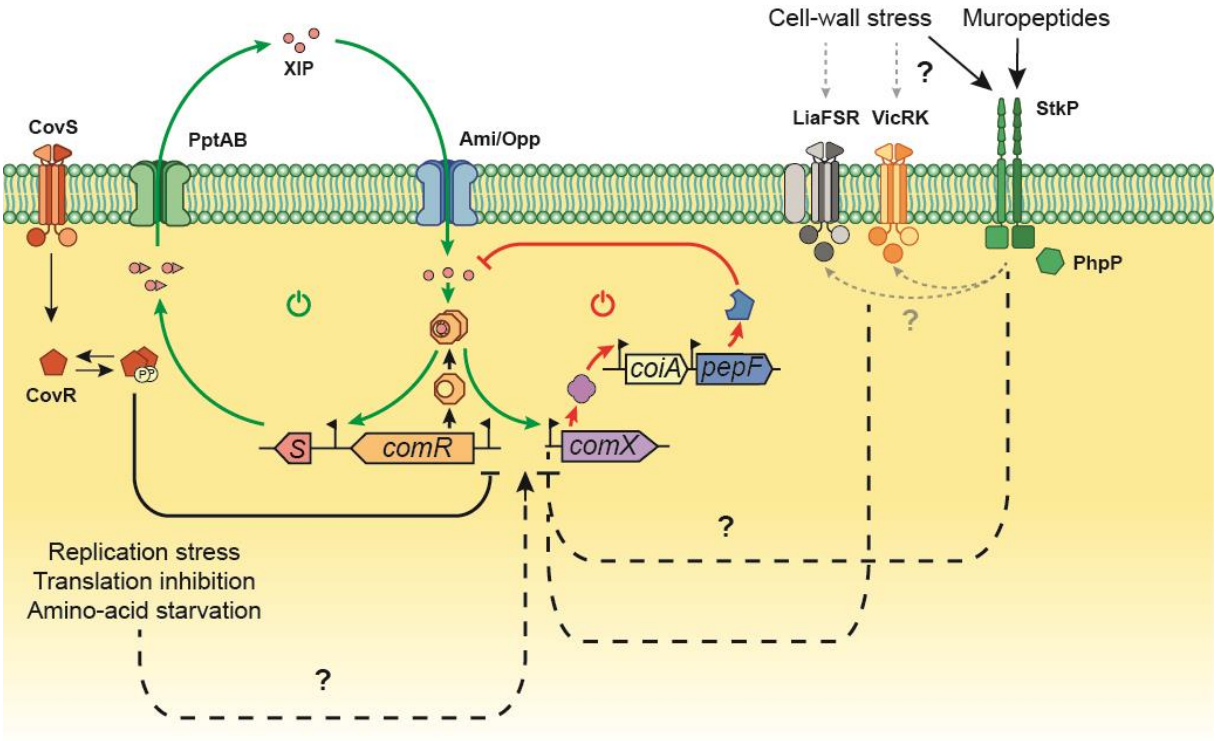

Figure 6. Model of competence regulation integrating cell-wall sensors and physiological stresses in *S. salivarius*. Upon CovRS repression release, ComR reaches a threshold concentration allowing the activation of a positive feedback loop (green arrows, power-on icon). The positive loop is triggered by XIP binding to ComR, producing the ComR•XIP complex which activates *comS* transcription. ComS is then exported by the transporter PptAB and maturated. The mature XIP pheromone can then enter the cell by the oligopeptide generic transporter Ami/Opp and bind ComR to enhance the loop. In parallel, the ComR•XIP complex will trigger the transcription of *comX*, encoding the central regulator of competence. This will activate all the late genes necessary for natural transformation including the *coiA-pepF* operon. PepF accumulation will result in XIP degradation, generating a negative feedback-loop (red arrows, power-off icon) on the ComRS system, ultimately leading to competence exit. In parallel, cell-wall stress and/or free muropeptides can be sensed by the serine-threonine kinase StkP, LiaFSR and VicRK to modulate the transcriptional activation of *comX*, most probably via interfering with the activity of the ComR•XIP complex. Other physiological stresses such as replication stress, translation inhibition or amino-acid starvation were also identified as conditions that could activate competence development.